Homogeneity analysis of sculptured thin films deposited in symmetric style through glancing angle deposition technique*

Wang Bin(王 斌)[a)b)], Qi Hong-Ji(齐红基)[a)†], Sun Wei(孙 卫)[a)b)], He Jun(何 骏)[a)b)], Zhao Jiao-Ling(赵娇玲)[a)b)], Wang Hu(王 虎)[a)b)], and Hou Yong-Qiang(侯永强)[a)b)]

[a)] *Key Laboratory of Materials for High Power Laser, Shanghai Institute of Optics and Fine Mechanics, Chinese Academy of Sciences, Shanghai* 201800, *China*

[b)] *University of Chinese Academy of Sciences, Beijing* 100049, *China*

(Received 10 March 2014; revised manuscript received 11 May 2014; published online 24 September 2014)

The symmetric deposition technique is often used to improve the uniformity of sculptured thin film (STF). In this paper, optical properties of STF with the columnar angles $\pm\beta$ are analyzed theoretically, based on the characteristic matrix method for extraordinary waves. Then, the transmittances of uniformity monolayer and bilayer STF in symmetrical style are calculated to show the effect of the bilayer structure on the optical properties of STF. The inhomogeneity of STF is involved in analyzing the differences in transmittance and phase retardation between monolayer and bilayer STF deposited in symmetric style. The results show that optical homogeneity of STF can be improved by depositing in symmetric style at the normal incidence, but it is not the same case as the oblique incidence.

Keywords: birefringence, dielectric thin films, optical properties

PACS: 78.20.Fm, 78.20.Ci, 42.25.Ja **DOI:** 10.1088/1674-1056/23/11/117801

1. Introduction

Anisotropy of crystalline molecules and unit cells[1,2] endows crystals with birefringent properties. However, the anisotropy of sculptured thin film (STF)[3–5] is induced by packing columns and the inclination of columnar structures.[6] Compared with crystals, STFs have the advantages of lower cost, efficiency, and almost unrestricted materials.[7–11] More importantly, the optical components can be easily enlarged based on the STF technique. Therefore, STFs have attracted a great deal of attention due to their optical properties.[12,13] Their applications are also greatly anticipated.[14] Numerous kinds of optical components with STF have been successfully manufactured, such as phase-retardation devices,[15] polarization-selective beam splitters,[16] polarizers,[17] sensors,[18] notch filters,[19,20] Fabry–Perot filters,[21] and three-dimensional (3D) photonic crystals.[22] For the glancing angle deposition technique (GLAD), the application of STF is normally limited by the uniformity of STF, which is ascribed to the difference in distance between substrate and evaporation source. To improve the uniformity of STF, Motohiro and Taga[6] proposed a symmetric deposition style to prepare the waveplate. Using this technique, Motohiro and Taga produced 60×250 mm uniform retardation plates with 3 μm thickness. The bilayer STF deposited in symmetric style showed improved homogeneity at the normal incidence. In fact, the two layers in the bilayer structure were not similar and inhomogeneous, even if their deposition angle was symmetric. In other words, bilayer STF deposited in symmetric style includes two different nonuniform single layers. Therefore, the inhomogeneity of STF should not be solved completely in symmetric deposition style, and relevant research is very helpful and meaningful.

In this research, we investigate the optical properties of uniform monolayer and bilayer STFs deposited in symmetric style, based on the characteristic matrix method for the extraordinary wave. The results demonstrate that the STFs show different optical responses for the columnar angles $\pm\beta$ at the oblique incidence. We further analyze the difference in optical property between nonuniform monolayer STF and inhomogeneous bilayer STF deposited in symmetric style with the same thickness nonuniformity. Our research provides some support for the design of large-sized uniform STF through the symmetric deposition style.

2. Theory and structure models of STF

2.1. Theory

In terms of optical properties, the anisotropic spacing of columns causes the biaxial birefringence to be characterized by an index n_1 along the columns, an index n_2 normal to the columns in the vapor incidence plane, and an index n_3 normal to the vapor incidence plane.[6] Like isotropic thin film, the characteristic matrix can be used to treat the anisotropic thin film in the case of incident plane consistent with the deposition plane in our previous publication.[23,24] The propagations of the TE wave (s-polarized wave) and the TM wave (p-polarized wave) are decoupled. The TE wave propagates

*Project supported by the National Natural Science Foundation of China (Grant No. 61205211).

†Corresponding author. E-mail: qhj@mail.siom.ac.cn

© 2014 Chinese Physical Society and IOP Publishing Ltd

across STF in an ordinary way, independent of the traveling direction. However, the TM wave propagates across the anisotropic thin film in an extraordinary manner. To analyze the inhomogeneity of STF through the symmetric deposition style, we study the difference between the optical properties of STFs with the same thickness and the incident angle, but different symmetric columnar angles.

In case of an s-polarized wave, the characteristic matrix can be written as[25]

$$\begin{bmatrix} \cos\delta_s & \frac{\mathrm{i}}{\eta_s}\sin\delta_s \\ \mathrm{i}\eta_s\sin\delta_s & \cos\delta_s \end{bmatrix}. \tag{1}$$

The optical properties are determined by the refractive index n_3, the refraction angle θ_s, and the physical thickness d of the film. $\eta_s = n_3\cos(\theta_s)$ and $\delta_s = \frac{2\pi}{\lambda}n_3 d\cos(\theta_s)$ refer to the effective optical admittance and the phase thickness, respectively. Thus, the optical properties of the birefringent thin film are similar to those of the isotropic thin film in the case of TE wave propagation. Therefore, we rarely consider the TE wave in STF.

In the case of a p-polarized wave, the 2×2 characteristic matrix of STF with the columnar angle of $+\beta$ and incident angle of θ_0 is derived as follows:

$$M = \frac{1}{\eta_+ + \eta_-} \times \begin{bmatrix} \eta_- \mathrm{e}^{\mathrm{i}\delta_+} + \eta_+ \mathrm{e}^{-\mathrm{i}\delta_-} & \mathrm{e}^{\mathrm{i}\delta_+} - \mathrm{e}^{-\mathrm{i}\delta_-} \\ \eta_-\eta_+(\mathrm{e}^{\mathrm{i}\delta_+} - \mathrm{e}^{-\mathrm{i}\delta_-}) & \eta_+\mathrm{e}^{\mathrm{i}\delta_+} + \eta_-\mathrm{e}^{-\mathrm{i}\delta_-} \end{bmatrix}, \tag{2}$$

where η_+ and η_- are the effective optical admittances of forward- and backward-traveling wave, and δ_+ and δ_- are the phase thickness for forward- and backward-traveling wave respectively. The symbols in this paper are in accordance with the convention in Refs. [23] and [24].

The input optical admittance $Y = C/B$ can be easily obtained from the following equation:

$$\begin{pmatrix} B \\ C \end{pmatrix} = M \begin{pmatrix} 1 \\ \eta_g \end{pmatrix}, \tag{3}$$

where η_g is the effect optical admittance of p-polarized wave in the substrate. According to the formula above, we derive the input optical admittance as

$$Y = \frac{C}{B} = \frac{\eta_+(\eta_g+\eta_-)\,\mathrm{e}^{\mathrm{i}\delta_+} + \eta_-(\eta_g-\eta_+)\,\mathrm{e}^{-\mathrm{i}\delta_-}}{(\eta_g+\eta_-)\,\mathrm{e}^{\mathrm{i}\delta_+} + (\eta_+-\eta_g)\,\mathrm{e}^{-\mathrm{i}\delta_-}}. \tag{4}$$

When the columnar angle turns into $-\beta$ at the incident angle of θ_0, the phase thickness values and the effective optical admittances of the forward and backward traveling wave vectors can be denoted by δ'_+, δ'_-, η'_+, and η'_-. These optical parameters may relate to those of the columnar angle of $+\beta$. Based on the reciprocal of the optical path, $\delta'_+ = \delta_-$, $\delta'_- = \delta_+$ and $\eta'_+ = \eta_-$, $\eta'_- = \eta_+$ can be obtained. Similarly, we derive the input optical admittance with the columnar angle of $-\beta$

$$Y' = \frac{C'}{B'} = \frac{\eta_+(\eta_g-\eta_-)\,\mathrm{e}^{-\mathrm{i}\delta_+} + \eta_-(\eta_g+\eta_+)\,\mathrm{e}^{\mathrm{i}\delta_-}}{(\eta_- - \eta_g)\,\mathrm{e}^{-\mathrm{i}\delta_+} + (\eta_+ + \eta_g)\,\mathrm{e}^{\mathrm{i}\delta_-}}. \tag{5}$$

Even with the same thickness and incident angle, the difference in optical admittance between the STF of the columnar angle $+\beta$ and that of $-\beta$ can be noticed clearly. As a consequence, the optical properties, such as the input optical admittance, transmittance and reflectance, are not identical with those for the case of extraordinary wave generally.

Under the normal incidence, the incident angle is $\theta_0 = 0^\circ$. Then, we can deduce the following equations:

$$\begin{cases} n(\alpha_1) = n(\alpha_2) = n(\alpha_1)' = n(\alpha_2)' = n, \\ n = \dfrac{1}{\left(\dfrac{\sin^2\beta}{n_1^2} + \dfrac{\cos^2\beta}{n_2^2}\right)^{1/2}}, \end{cases} \tag{6}$$

$$\begin{cases} \eta'_+ = \eta_- = \eta'_- = \eta_+ = \eta, \\ \eta = n, \end{cases} \tag{7}$$

$$\begin{cases} \delta_+ = \delta_- = \delta'_+ = \delta'_- = \delta = \dfrac{2\pi}{\lambda}d, \\ Y = Y' = \dfrac{C}{B} = \dfrac{\eta(\eta_g-\eta)\,\mathrm{e}^{-\mathrm{i}\delta} + \eta(\eta_g+\eta_+)\,\mathrm{e}^{\mathrm{i}\delta}}{(\eta-\eta_g)\,\mathrm{e}^{-\mathrm{i}\delta} + (\eta+\eta_g)\,\mathrm{e}^{\mathrm{i}\delta}}. \end{cases} \tag{8}$$

Evidently, STFs with columnar angles $+\beta$ and $-\beta$ have the same optical properties at the normal incidence. The symbols above are cited from Refs. [23] and [24].

Based on the above analysis of the characteristic matrix for TM wave, STFs can be regarded as the same or different media for the columnar angles $+\beta$ and $-\beta$ at the normal incidence or oblique incidence, respectively. Our results can be expanded into multilayer films. For the multilayer films, the input optical admittance can be deduced using

$$\begin{bmatrix} B \\ C \end{bmatrix} = M_n M_{n-1}\cdots M_2 M_1 \begin{bmatrix} B \\ C \end{bmatrix} = M \cdot \begin{bmatrix} 1 \\ \eta_g \end{bmatrix},$$

where M_n is the characteristic matrix of the n-layer film.

2.2. Structure models of STF

In order to analyze the inhomogeneity of STF in symmetric deposition style as shown in Fig. 1(d), four structure models are used to investigate the optical properties of STF at the normal and oblique incidences. The principle refractive indices of Ta_2O_5 deposited by GLAD in our previous work[26,27] are $n_1 = 1.81$, $n_2 = 1.74$, and $n_3 = 1.78$. The symbols M and N refer to the 100-nm physical thickness anisotropic Ta_2O_5 STFs with column angles of 60° and –60° respectively. The incident and emergent media are homogeneous isotropic air and glass substrate, which are denoted by A and G.

For the uniform monolayer STF, the stack structure can be written as G/2M/A. It can be described as 2M as shown in Fig. 1(a). For comparison, the MN model is used to describe

the uniform bilayer STF. The stack structure is G/MN/A, as shown in Fig. 1(b).

As mentioned above, the uniformity of STF is not good due to different distances between the surface of the substrate and the evaporation source. The nonuniformity can almost reach 10% for the STF with a 50 mm diameter in our previous experiments. In order to obtain 90° phase retardation in the visible range, [28] the thickness of STF is about several microns generally. Therefore, nonuniform monolayer STFs (IMSs) with different thickness values ranging from 1820 nm to 2180 nm are constructed as shown in Fig. 1(c). Based on calculation results, the nonuniform monolayer STF can be equivalent to a sufficient number of uniform monolayer STFs, and the final optical properties can be regarded as the integral of those over the entire surface of STFs. The thin films can be written as 18.2M to 21.8M.

To improve the uniformity of anisotropic thin film, inhomogeneous bilayer STF (IBS) deposited in symmetry style could be represented with two layers of nonuniform STF, as shown in Fig. 1(d). The second layer is equal to the first layer rotated 180 degrees with respect to the normal angle of the incident plane. For comparison, the same thickness is used in the calculation. Like IMS, the final optical properties can be regarded as the integral of those over the entire surface of STFs. The stack of the thin film can be written as G/9.1M10.9N/A on the left side, G/10.9M 9.1N/A on the other side, and G/10M10N/A at the center of the substrate.

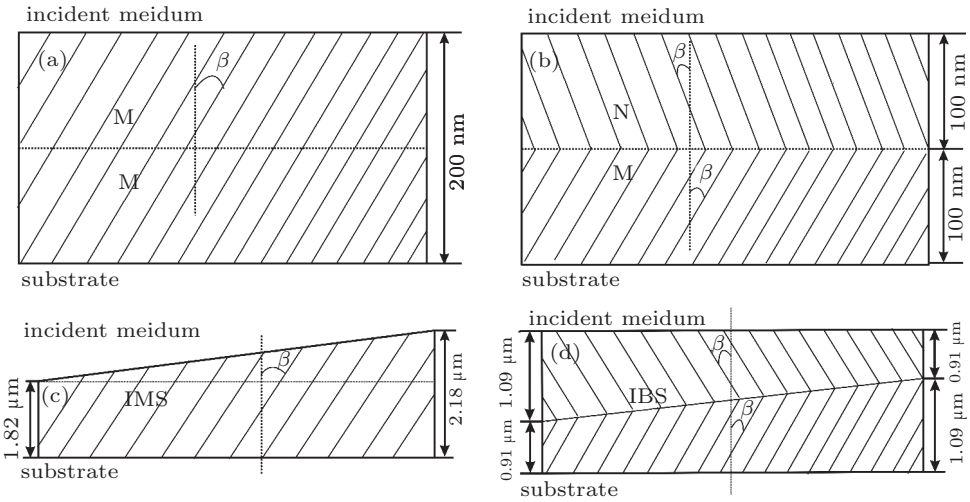


Fig. 1. Schematic diagrams of the four model structures: (a) 2M, (b) MN, (c) IMS, and (d) IBS.

3. Results and discussion

First of all, we discuss the difference in optical property between 2M and MN structure models, as shown in Figs. 1(a) and 1(b), respectively. The TM and TE transmission spectra of 2M and MN structures at the normal incidence are described in Fig. 2 in a region from 300 nm to 800 nm. It is not surprising to find that the transmittance spectra of a TE wave are completely overlapped for 2M and MN structures. However, it also yields the same phenomenon as that for the case of a TM wave. The phenomenon indicates, under the normal incidence, 2M and MN have an identical characteristic matrix. It means that M and N can be regarded as the identical medium, and there is no difference between 2M and MN under the normal incidence condition.

The TM transmission spectra of 2M and MN structures at the oblique incidence are plotted in Fig. 3(a). It can be clearly shown that the transmittance spectra of 2M and MN are separated from each other and shift toward the short wavelength at the oblique incidence. It indicates that M and N cannot be regarded as the same materials at the oblique incidence, which is not the same as the scenario at the normal incidence as indicated by the above theoretical analysis results. It is interesting to note that the transmittance spectra for 2M and MN almost overlap with each other near the wavelength of 325 nm. The equivalent optical thickness of the M or N layer almost equals 162.5 nm, which can be regarded as quarter-wave optical thickness (QWOT) at the wavelength of 650 nm. Therefore, the M and N layers show half-wave optical thickness (HWOT) at the wavelength of 325 nm. That is to say, both the MN and 2M stack structures correspond to the absentee layer at 325 nm, and the transmittance is the same as that of an uncoated substrate. In order to make a further investigation of this point, the basic structure MN is repeated several times, and the calculated transmission spectra are plotted in Figs. 3(b) and 3(c). The details of variation with the repeating times can be seen in Fig. 3(d), clearly. At a wavelength of 650 nm, TM transmittance declines rapidly with the number of periods increasing. It can be explained by the fact that M and N are different materials , i.e., the high and low index materials with 180° phase shift, and can be regarded as the basic reflective unit.

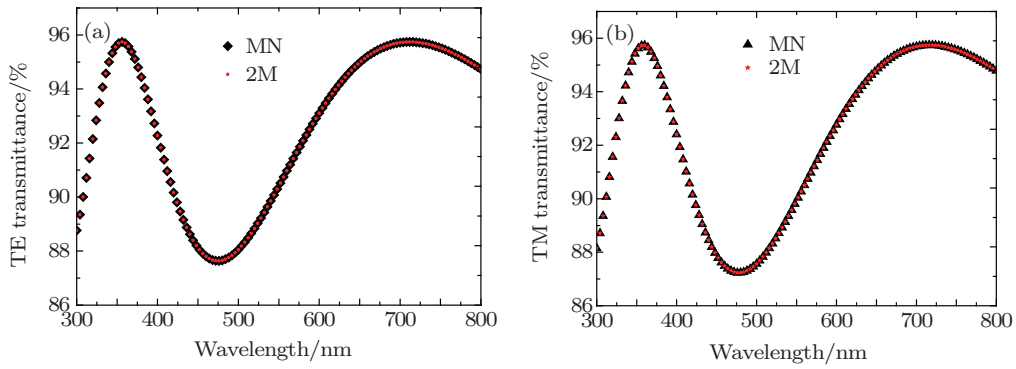


Fig. 2. (color online) Transmission spectra of MN and 2M at normal incidence for (a) TE and (b) TM.

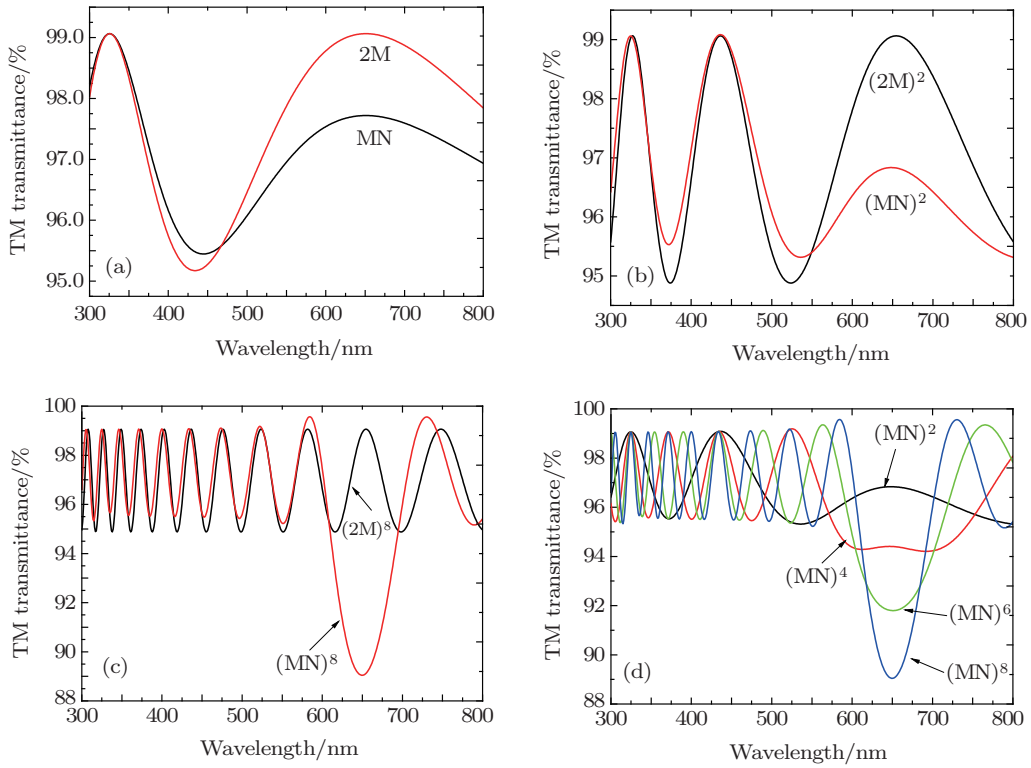


Fig. 3. (color online) TM transmittance spectra of (a) MN and 2M, (b) $(2M)^2$ and $(MN)^2$, (c) $(2M)^8$ and $(MN)^8$, and (d) $(MN)^2$, $(MN)^4$, $(MN)^6$, $(MN)^8$ at 45° oblique incidence.

In view of the calculation of transmittance for 2M and MN, the results of our theoretical analysis are confirmed. At the normal incidence, M and N can be equivalent to the same materials. In the case of oblique incidence, M and N must be different media.

Although there exists an interface between M and N in IBS, the interface could be ignored because M and N can be regarded as identical materials at the normal incidence. Therefore, we predict that the inhomogeneity of STF can be modified in the symmetric deposition style at the normal incidence. In the case of IMS, the transmittance of TM wave is shown in Fig. 4(a) at normal incidence with thickness values of 21.8M and 18.2M. The nonuniformity of thickness induces obvious spectral shift. Nevertheless, for the IBS deposited in symmetric style, no spectral shift is shown in Fig. 4(b) for the MN structure model at the normal incidence. It implies that the inherent inhomogeneity of STF induced by the GLAD technique can be improved through the symmetric deposition style. This information provides theoretical support for the high-homogenity design of STF at the normal incidence with the symmetric deposition trick.

Under the oblique incidence, M and N are different media, so we predict that the optical inhomogeneity of STF will still exist even in the case of the symmetric deposition style at the oblique incidence. TM transmittance spectra and phase retardation of IMS and IBS at 45incidence are investigated. Three sets of stacks representing the different STF structures on the substrate surface are calculated. Nonuniformity of IMS

induces clearly a wavelength shift as shown in Figs. 5(a) and 5(b). The phase retardation of IMS can be positively correlated with the thickness. Compared with those presented in Figs. 5(a) and 5(b), wavelength shift can be reduced greatly for the IBS structure model in Figs. 5(c) and 5(d), but the amplitudes of transmittance and phase retardance depend on the thickness values of M and N layers. We can obtain that the phase retardation of IBS becomes smaller than that of IMS. The reason for this phenomenon is that M and N, as the different media due to the different refractive indices of the TM wave, have the opposite phase retardation effects, thereby reducing the phase delay of IBS. These results validate our analysis results, showing that the optical inhomogeneity would still exist even after adopting the symmetric deposition style at oblique incidence.

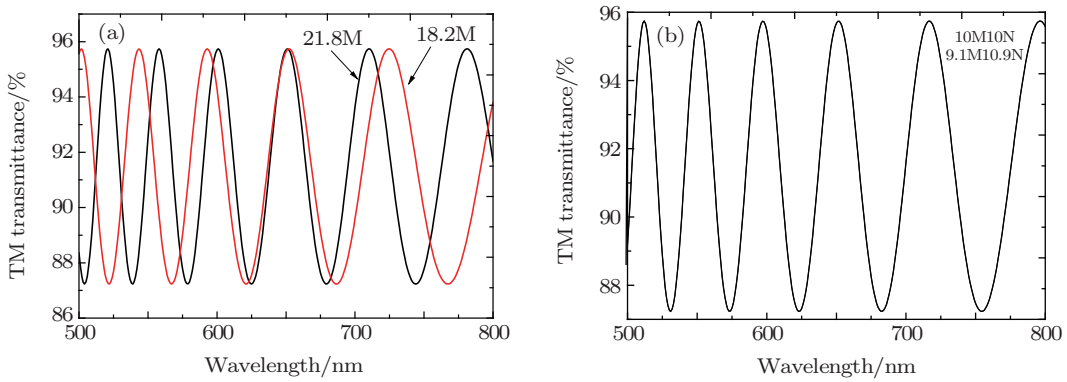


Fig. 4. (color online) TM transmittance spectra of (a) IMS and (b) IBS at normal incidence.

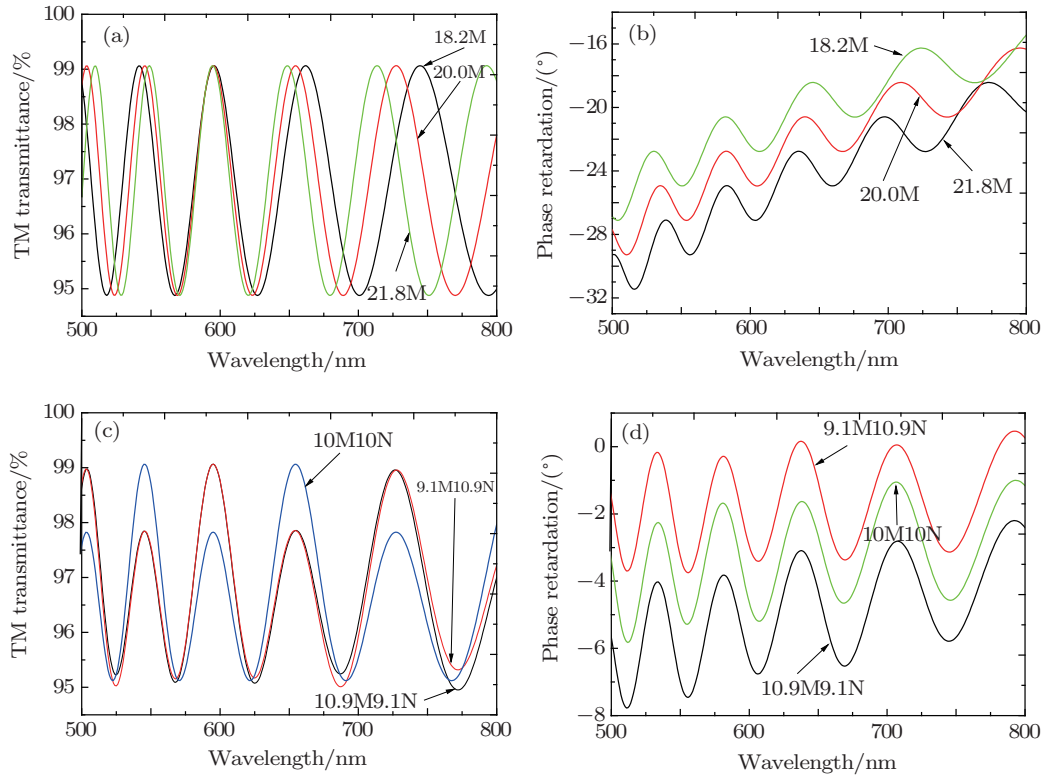


Fig. 5. (color online) The TM transmittance and phase retardation spectra for ((a), (b)) IMS and ((c), (d)) IBS at 45° incidence.

4. Conclusion

In this paper, uniform monolayer STF and bilayer STF deposited in the symmetric style with the same thickness values are investigated with the developed software package based on the characteristic matrix method. STFs can be regarded as identical or different media for the columnar angles $+\beta$ and $-\beta$ at normal incidence and oblique incidence, re-

spectively. The research results support the design of adopting the symmetric deposition style to modify the inhomogeneity of STF at normal incidence. In the case of oblique incidence, bilayer STF deposited in symmetric style could mitigate the problem of the wavelength shift due to thickness nonuniformity. However, optical inhomogeneity would still exist. In summary, the conclusion provides new support for the design of large-sized homogeneous STF through the symmetric deposition style.

References

[1] Wan Y T, Hu H Y, Xia H P, Zhang Y P, Jiang H C and Chen H C 2012 *Chin. Opt. Lett.* **10** 042301
[2] Li L, Fu L, Xu X, Zhai J and Ruan S 2012 *Chin. Opt. Lett.* **10** 311601
[3] Robbie K, Brett M J and Lakhtakia A 1996 *Nature* **384** 616
[4] Macleod H A 2010 Thin-Film Optical Filters (4th edn.) (Boca Rotan: CRC) pp. 13–57
[5] Hodgkinson I J, Hazel J C and Wu Q H 1998 *Thin Solid Films* **313** 368
[6] Motohiro T and Taga Y 1989 *Appl. Opt.* **28** 2466
[7] Siabi-Garjan A, Savaloni H, Abdi F, Ghaffal A and Placido F 2013 *Phys. Script.* **87** 055705
[8] Cao S P, Ye F, Hou B and Xu A Y 2013 *Thin Solid Films* **545** 205
[9] Singh D P, Goel P and Singh J P 2012 *J. Appl. Phys.* **112** 104324
[10] Xiao X D, Dong G P, Shao J D, He H B and Fan Z X 2010 *Appl. Surf. Sci.* **256** 1636
[11] Wang S M, Xia G D, Fu X, He H B, Shao J D and Fan Z X 2007 *Thin Solid Films* **515** 3352
[12] Hou Y Q, Qi H J, Yi K and Shao J D 2013 *Chin. Opt. Lett.* **11** 103101
[13] Fu X Y, Wang S M, Deng D G, Yi K and Fan Z X 2006 *Chin. Opt. Lett.* **4** 247
[14] Qi H J, Wang J P, Erdmann A, Jin Y X, Shao J D and Fan Z X 2010 Seventh International Conference on Thin Film Physics and Applications, September 24, 2010 Shanghai, China p. 799519
[15] Hou Y Q, Li X, He K, Qi H J, Yi K and Shao J D 2013 *Chin. Phys. Lett.* **30** 017802
[16] Qi H J, Hong R J, Yi K, Shao J D and Fan Z X 2005 *Appl. Opt.* **44** 2343
[17] Fu X Y, Yi K, Shao J D and Fan Z X 2008 *Chin. Opt. Lett.* **6** 544
[18] Lakhtakia A and Messier R 2005 Sculptured Thin Films: Nanoengineered Morphology and Optics (Vol. PM143) (Washington: SPIE press)
[19] Hodgkinson I J, Wu Q H, Lakhtakia A and McCall M W 2000 *Opt. Commun.* **177** 79
[20] Pursel S M, Horn M W and Lakhtakia A 2007 *Opt. Eng.* **46** 040507
[21] Qi H J, Hou Y Q, Yi K and Shao J D 2013 *J. Opt. Soc. Korea* **17** 33
[22] Venugopal V C 2013 *J. Nanophoton.* **7** 073502
[23] Qi H J, Zhang D P, Shao J D and Fan Z X 2005 *Europhys. Lett.* **70** 257
[24] Qi H J, Shao J D and Fan Z X 2007 *Europhys. Lett.* **78** 17004
[25] Qi H J, Zhu M P, Zhang W L, Yi K, He H B and Shao J D 2012 *Chin. Opt. Lett.* **10** 013104
[26] Qi H J, Xiao X D, He H B, Yi K and Fan Z X 2009 *Appl. Opt.* **48** 127
[27] Xiao X D, Dong G, He H B, Qi H J, Fan Z X and Shao J D 2009 *Chin. Opt. Lett.* **7** 967
[28] Hou Y Q, Qi H J, Li X, He K, Yi K and Shao J D 2013 *Chin. Phys. B* **22** 127801